Electrical Properties of Low Density Polyethylene/ZnO Nanocomposites: The Effect of Thermal Treatments

S. C. Tjong, G. D. Liang, S. P. Bao

Department of Physics and Materials Science, City University of Hong Kong, Tat Chee Avenue, Kowloon, Hong Kong

Received 1 December 2005; accepted 10 February 2006
DOI 10.1002/app.24294
Published online in Wiley InterScience (www.interscience.wiley.com).

ABSTRACT: Low density polyethylene (LDPE)/ZnO nanocomposites were prepared by melt compounding followed by annealing or quenching treatment. Electrical properties of the thermally treated nanocomposites were investigated. The results showed that thermal treatments exerted a pronounced effect on the electrical properties of LDPE/ZnO nanocomposites. The dielectric constant of annealed LDPE/ZnO nanocomposites at various ZnO contents was higher than that of quenched nanocomposites. In sharp contrast, the resistivity of annealed LDPE/ZnO nanocomposites was considerably lower than that of quenched samples. The frequency dependence of dielectric constant was much pronounced for both the annealed and quenched LDPE/ZnO nanocomposites associated with the formation of ZnO network as the ZnO volume content reached 52 vol %. The structure–property relationship of the nanocomposites is discussed. © 2006 Wiley Periodicals, Inc. J Appl Polym Sci 102: 1436–1444, 2006

Key words: low density polyethylene; dielectric constant; resistivity; crystallization

INTRODUCTION

Polymers are regarded as insulating materials because of their low conductivity. The electrical properties of the insulating polymers can be modified by adding conductive particles such as carbon nanotube,[1–3] metallic filler,[4,5] and ZnO.[6–8] The electrical properties of the composites depend greatly on the conducting filler distribution within the polymer matrix. For low filler concentration, the fillers in the form of small particles distribute homogeneously in the insulating polymer host. With increasing filler content, agglomeration of filler particles begins to form. At a certain filler content, the growing agglomerates appear to contact each other, leading to the formation of a one-, two-, or three-dimensional network of the conducting phase within the insulating host. As a result, the electrical conductivity of the composites shows a drastic increase from low to high value of the conductive network.[9] This phase transition from respective small isolated cluster to infinite interconnected network is referred to as percolation transition.[10]

ZnO is a semiconducting oxide with a wide and direct bandgap of 3.4 eV and a large exciton binding energy of 60 meV.[11] Accordingly, ZnO is an important electronic and photonic material for UV light-emitters, varistors, gas sensors, acoustic wave devices, etc.[12–14] Recently, ZnO nanoparticles have attracted considerable attention because of the unique physical properties and their potential applications in nanodevices. Several studies have been conducted on the synthesis and the structure–property of ZnO nanoparticles.[15–17] Semiconductor nanoparticles embedded in a polymer matrix have recently been considered as biosensors for the detection of species in biofluids.[18] The synthesis, morphology, and optical properties of ZnO particle-polymer thin films have also been reported more recently. These nanocomposite hybrid films were prepared via polymerization reactions.[19,20] In practices, it is cost effective to prepare large volume nanocomposites by melt blending process.

Crystallization behavior of polymers and their composites play a crucial role on morphologies and the resulting properties to some extent.[21–24] Crystallization is regarded as a naturally self-assembly process.[25] In the process, the filler particles and other impurities in the composites are rejected from the crystal phase and incorporated into the amorphous region.[24] Recently, Zheng et al. investigated the structure and morphology of the polyamide-6/ZnO nanocomposites. They reported that the ZnO nanoparticles can induce the crystallization of the γ-crystalline form PA-6 from the melt and during the annealing of the amorphous solid.[26]

In this article, low density polyethylene (LDPE)/ZnO nanocomposites are prepared by melt compounding and the effect of thermal treatments on their electrical properties is investigated. The structure–property relationship of such nanocomposites is dis-

Correspondence to: S. C. Tjong (aptjong@cityu.edu.hk).

cussed. The dependence of electrical properties of the LDPE/ZnO nanocomposites on thermal treatments is related to crystallization of the nanocomposites.

EXPERIMENTAL

Sample preparation

LDPE/ZnO composites were prepared by melt-blending commercial LDPE with ZnO particles in a Brabender mixer. The LDPE (Cosmothene LDPE G812) with a density of 0.917 g cm^{-3} was supplied by Polyolefin, Singapore. The melt-flow index of LDPE (2.16 kg, 190°C) was 35 g $(10\ min)^{-1}$. No additives were added in LDPE. ZnO nanoparticles of ~200 nm with 99.9% purity were supplied by Nanostructured and Amorphous Materials (Los Alamos, NM). To disperse the ZnO particles into the polymer matrix more uniformly and to avoid thermal degradation of the polymer matrix, the mixing time was set to 15 min at 120°C. The blended mixtures were then hot pressed at 200°C under 10 MPa into plates of 1 mm. Disk samples of 12 mm diameter and 1 mm thickness were punched from these plates. To avoid the effect of moisture on electrical properties, all the disk samples were stored in desiccators prior to electrical properties measurements. Annealing of the samples was performed at a 50°C for 50 h. Quenching was conducted by rapidly dropping the molten samples (200°C) into ice water. The cooling rate was estimated exceeds 1000°C min^{-1}.

Electrical properties

Samples for the dielectric and resistivity measurements were coated with silver paint prior to the tests. Two metallic electrodes were then connected to the samples using silver wires. The dielectric constant and resistivity of samples were measured by employing an impedance analyzer (Agilent model 4294) in the frequency range of 40–10^7 Hz at room temperature.

X-ray diffraction

X-ray diffraction (XRD) measurements were performed with a Philip X'pert diffractometer equipped with Ni-filtered Cu Kα radiation, having a wavelength of 0.154 nm. The diffractometer was scanned in 2θ range of 5–40 ° and the scanning rate used was 1.2° min^{-1}.

Differential scanning calorimetry

Melting behavior of LDPE/ZnO nanocomposites was investigated with a TA Instruments DSC (model 2910) under a nitrogen atmosphere. The LDPE/ZnO nanocomposites (about 5 mg) were sealed in aluminum pans. The samples were heated to 180°C at a rate of 10°C/min. The change of heat flow versus time was recorded.

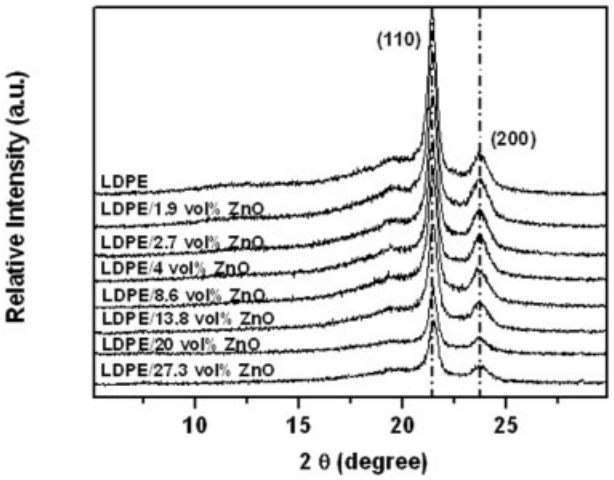

Figure 1 XRD patterns of as-prepared LDPE/ZnO nanocomposites.

Polarizing optical microscopy

The crystalline morphology of LDPE and its nanocomposites was observed with a polarizing optical microscope (Olympus BH2-UMA) equipped with a camera (Olympus DP 11). The samples were sandwiched between two microscopic glass slides and then mounted on a hot stage. They were held at 200°C for 5 min to eliminate thermal history and pressed into thin film of ~0.1 mm thickness and slowly cooled to room temperature.

Scanning electron microscopy

The microstructure of samples was examined by scanning electron microscopy (SEM, JEOL JSM model 820). The samples for SEM examination were fractured in liquid nitrogen. They were coated with a thin layer of gold prior to SEM observation.

RESULTS AND DISCUSSION

XRD technique is a powerful method to determine the structure of LDPE/ZnO nanocomposites. Figure 1 shows the XRD curves of as-prepared LDPE/ZnO nanocomposites. The XRD patterns of LDPE and its nanocomposites show two distinct (110) and (200) reflection peaks associated with the orthorhombic structure of LDPE. A broad shoulder located at ~19.3 ° is observed next to the (110) peak. The crystalline peaks of polyethylene can be discerned from the amorphous region by the deconvolution profile fitting. Figure 2 shows the representative profile fitting curve for the XRD pattern of LDPE/ZnO nanocomposite. From Fig-

ure 2, some parameters such as full width at half maximum (FWHM) and degree of crystallinity can be obtained. FWHM of crystalline peaks such as (110) and (200) of polyethylene, i.e., FWHM (110) and FWHM (200), can be employed to describe the perfectness of polyethylene crystals in LDPE/ZnO nanocomposites. Figures 3(a) and 3(b) show the variation of FWHM (110) and FWHM (200) of LDPE/ZnO nanocomposites with ZnO volume content, respectively. It is observed that FWHM (110) and FWHM (200) of as-prepared LDPE/ZnO nanocomposites increase slightly with the increase of ZnO content, respectively, showing that polyethylene crystals become less perfect as the ZnO content increases. Comparing with the FWHM (110) and FWHM (200) of as-prepared LDPE/ZnO nanocomposites, the quenched LDPE/ZnO nanocomposites exhibit higher FWHM (110) and FWHM (200), while the annealed samples show lower FWHM (110) and FWHM (200), indicating that the annealed LDPE/ZnO nanocomposites possess more perfect crystals than the quenched samples.

The degree of crystallinity (X_c) of polyethylene in the LDPE/ZnO nanocomposites can be determined from the integral of crystalline and amorphous peaks of polyethylene using the following equation.[27]

$$X_c = \frac{I_{110} + 1.46I_{200}}{I_{110} + 1.46I_{200} + 0.75I_a} \times 100\% \qquad (1)$$

where I_{110}, I_{200}, and I_a are the integral area of (110) and (200) crystal planes as well as the amorphous region of polyethylene, respectively. The degree of crystallinity of the as-prepared, annealed, and quenched LDPE/ZnO nanocomposites versus ZnO content is shown in Figure 3(c). It is apparent that the X_c of polyethylene in LDPE/ZnO nanocomposites decreases slightly with increasing ZnO content. It is observed that the X_c of

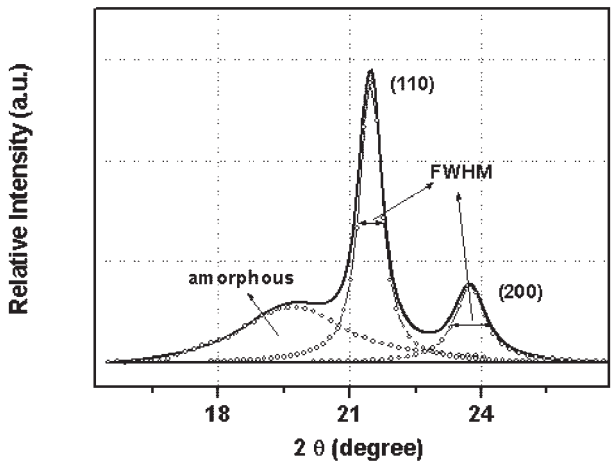

Figure 2 Reprensentative profile fitting for the XRD pattern of LDPE/ZnO nanocomposites.

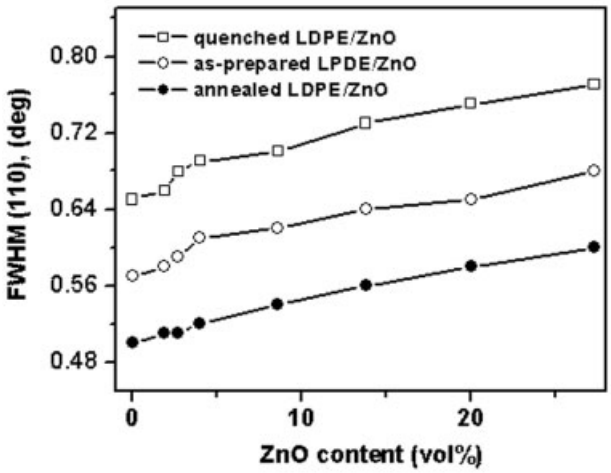

(a)

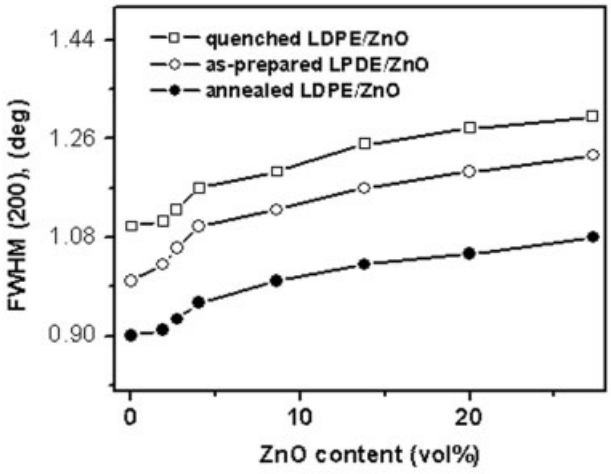

(b)

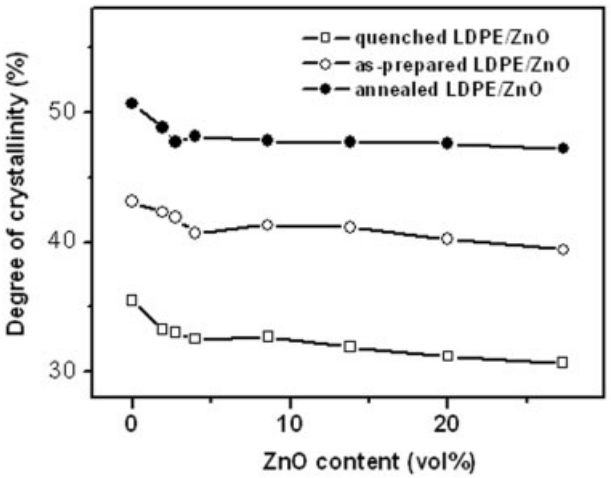

(c)

Figure 3 (a) FWHM (110), (b) FWHM (200) crystalline peaks, and (c) degree of crystallinity versus ZnO content for the LDPE/ZnO nanocomposites.

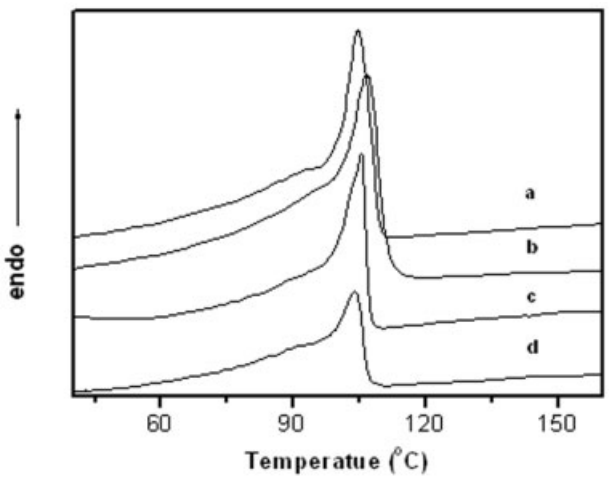

Figure 4 DSC curves of LDPE and LDPE/8.6 vol % ZnO nanocomposites. (a) neat LDPE, (b) annealed, (c) as-prepared, and (d) quenched LDPE/8.6 vol % ZnO nanocomposite specimens.

LDPE/ZnO nanocomposites is greatly affected by the thermal treatments. Comparing with the X_c of as-prepared LDPE/ZnO nanocomposites, quenched LDPE/ZnO nanocomposites exhibits lower X_c, but annealed LDPE/ZnO nanocomposites yields higher X_c. This is attributed to the annealed nanocomposites having more perfect crystals than the quenched samples.

For the purpose of comparison, the degree of crystallinity is also determined from differential scanning calorimetry (DSC) measurements. Figure 4 shows typical DSC scans for the as-prepared, annealed, and quenched LDPE/8.6 vol % ZnO nanocomposites specimens. The X_c of these samples can be determined using the following equation:

$$X_c = \frac{\Delta H_f}{\Delta H_f^0 (1 - w)} \times 100\% \qquad (2)$$

where ΔH_f is fusion enthalpy (J/g), ΔH_f^0 is fusion enthalpy of ideal PE crystals, being 295.8 J g^{-1}, and w is weight fraction of ZnO particles. The DSC results of the specimens investigated are presented in Figure 5. Comparing with Figure 3(c), it is apparent that the X_c values determined from DSC measurement are lower than those determined from the XRD technique. This is because the X_c value is strongly dependent on the measurement methodology. For instance, the ordered structure of PE crystals detected by the XRD instrument would not contribute to the fusion enthalpy in DSC scan.

Polarizing optical microscope is used to observe the spherulite morphology of LDPE and LDPE/8.6 vol % ZnO nanocomposite. Figure 6(a) shows the POM micrograph of pure LDPE. Perfect banded spherulites of LDPE resulted from periodic folding of crystalline lamellar is observed. The size of LDPE spherulites becomes smaller for LDPE/8.6 vol % ZnO nanocomposites as expected [Fig. 6(b)]. Annealing the LDPE/8.6 vol % ZnO nanocomposite leads to compacted spherulite morphology [Fig. 6(c)]. In contrast, spherulite structure is obscured in quenched LDPE/8.6 vol % ZnO nanocomposite [Fig. 6(d)], indicating that the crystal structure of quenched LDPE/8.6 vol % ZnO nanocomposites is less perfect.

Figure 7 shows the dielectric constant of as-prepared and thermally treated LDPE/ZnO nanocomposites as a function of ZnO content. For as-prepared LDPE/ZnO nanocomposites, the dielectric constant increases gradually with increasing ZnO content up to 60 vol %. There is no abrupt increase in the dielectric constant with ZnO content, known as percolation phenomenon, occurs for these composites even when ZnO volume fraction reaches 60 vol %. This is possibly due to the low dielectric property of ZnO (static dielectric constant of ZnO is about 8.7). This behavior is very different from that observed in polymer/high dielectric filler (such as carbon nanotube) composite in which percolation threshold exist.[3] In most polymer/filler composites, cluster structure is formed resulting from the agglomeration of filler particles at percolation threshold. Such a structure is favorable for the formation of filler cluster at relatively lower filler volume fraction.[10] From this, it becomes apparent that the fillers of LDPE/ZnO nanocomposites containing lower ZnO volume content are dispersed as isolated particles in the matrix rather than agglomeration of clusters. Figure 8(a) shows a typical SEM micrograph of the cryogenic fracture surface of the as-prepared LDPE/20 vol % ZnO nanocomposite. ZnO particles are observed as white particles dispersed throughout the matrix of the nanocomposite. A higher magnifica-

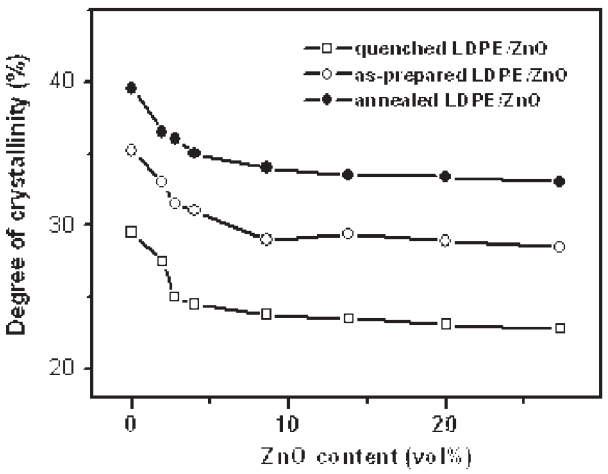

Figure 5 Degree of crystallinity versus ZnO content for the LDPE/ZnO nanocomposites determined from DSC measurements.

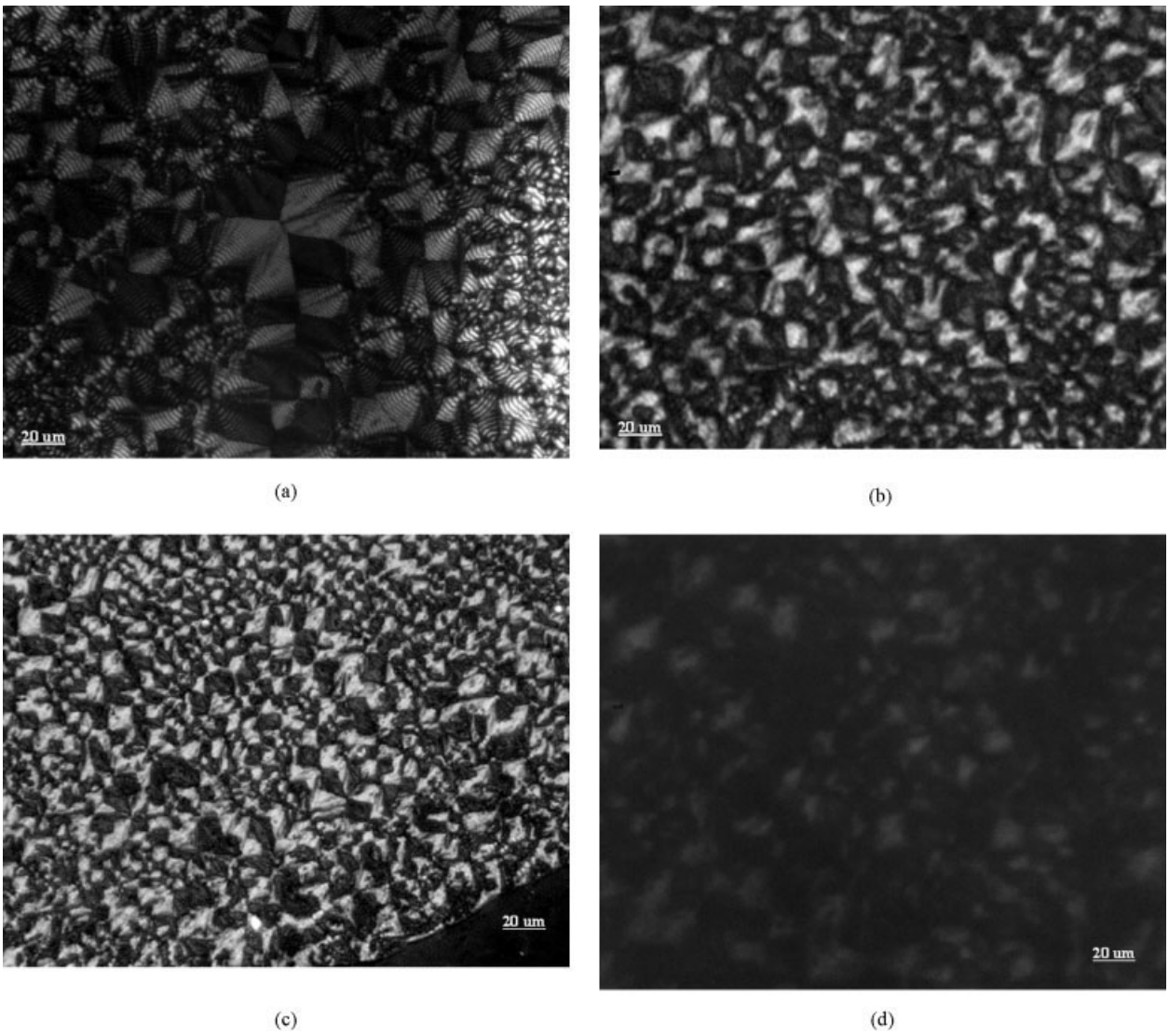

Figure 6 Polarizing optical micrographs of (a) neat LDPE, (b) as-prepared LDPE/8.6 vol % ZnO nanocomposites, (c) annealed LDPE/8.6 vol % ZnO nanocomposite samples, and (d) quenched LDPE/8.6 vol % ZnO nanocomposites specimens.

tion SEM reveals that ZnO particles are indeed dispersed as discrete particles in the polymer matrix [Fig. 8(b)].

From Figure 7, it can also be seen that thermal treatments have a profound effect on the dielectric constant of LPDE/ZnO nanocomposites. Annealed LDPE/ZnO nanocomposites exhibit higher, but quenched samples show lower dielectric constant. It is known that the electrical properties of crystalline polymers are greatly affected by their morphology, which is related to the thermal treatment process in turn.[24] Annealing LDPE/ZnO nanocomposites allows the polyethylene segments to have more time to fold into the crystalline lamellae, resulting in more perfect crystal structure. During crystallization process of polyethylene, ZnO particles, uncrystallizable macromolecuar chains, and other impurities (such as ionic species due to remaining catalyst, additives, etc.) are

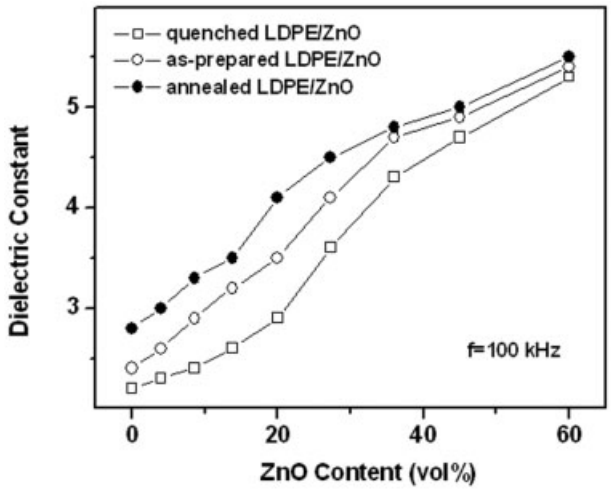

Figure 7 Plots of dielectric constant of as-prepared, annealed, and quenched LDPE/ZnO nanocomposites versus ZnO volume content.

rejected out of the crystalline structure, and finally incorporated into the amorphous region near the spherulites. This favors formation of the ZnO clusters and thereby promoting higher dielectric constant. For the quenched LDPE/ZnO nanocomposites, polyethylene segment has little time to fold into crystalline lamellae. The degree of crystallinity of quenched LDPE/ZnO nanocomposites is reduced, and the dielectric constant becomes smaller accordingly. More interestingly, the effect of thermal treatments on the dielectric constant of LDPE/ZnO nanocomposites is more pronounced at lower ZnO loading (<36 vol %). At high ZnO loading (>40 vol %), the respective polyethylene content in LDPE/ZnO nanocomposites is relatively reduced and the effects of thermal treatments and crystallization of polyethylene on the dielectric constant diminish.

Resistance is another crucial parameter for the application of polymeric composites in electronic industries. Figure 9(a) shows the resistivity at lower frequency region (50 Hz) of as-prepared, annealed, and quenched LDPE/ZnO nanocomposites, ρ, as a function of ZnO volume content. For as-prepared LDPE/ZnO nanocomposites, the resistivity remains un-

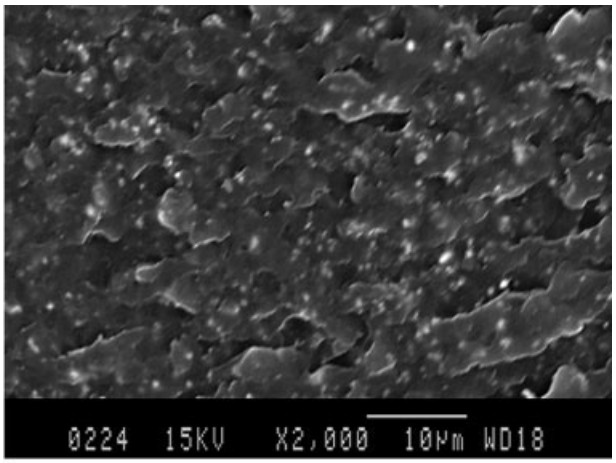

(a)

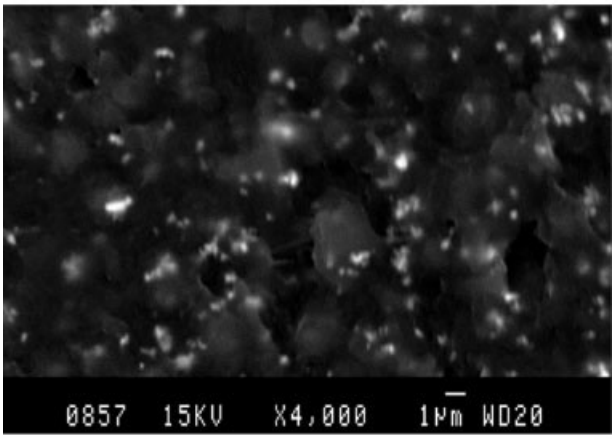

(b)

Figure 8 (a) Low and (b) high magnification SEM micrographs of cryogenic fracture surfaces of as-prepared LDPE/20 vol % ZnO nanocomposite.

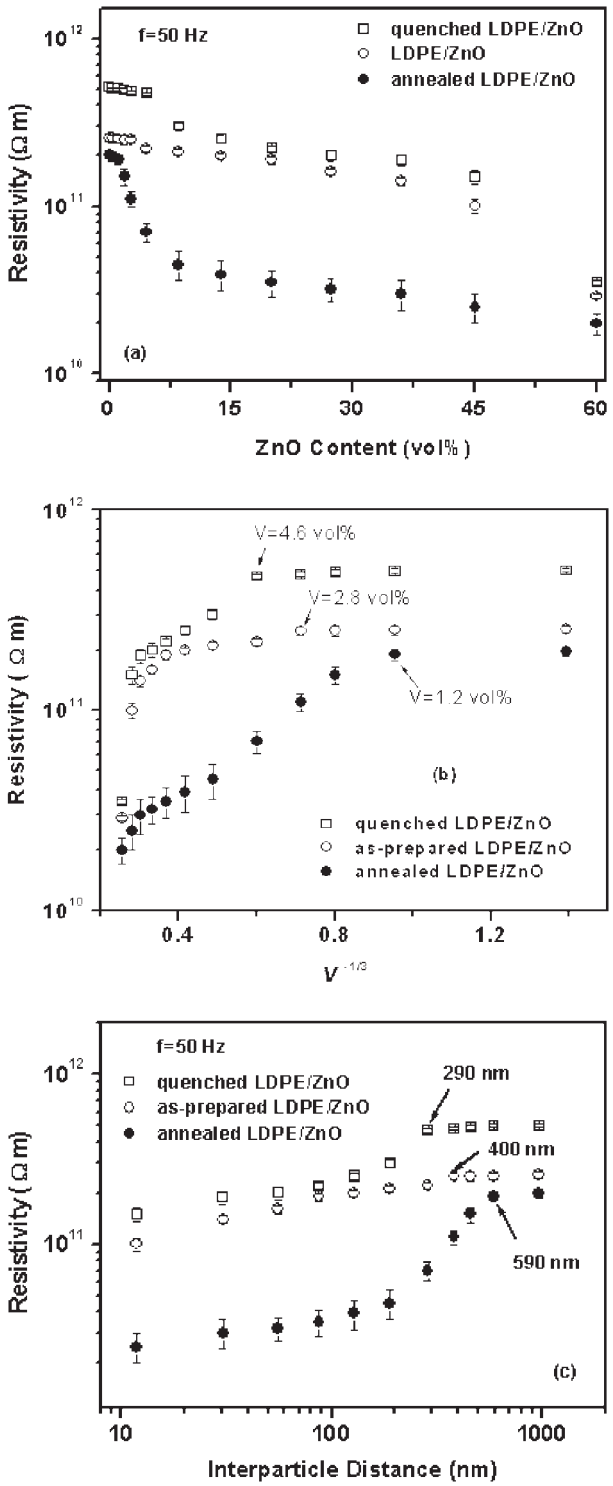

Figure 9 Plots of resistivity at lower frequency (50 Hz) of as-prepared, annealed, and quenched LDPE/ZnO nanocomposites versus (a) ZnO volume content, (b) $V^{-1/3}$, and (c) interparticle distance.

changed with the additions of ZnO up to 2.8 vol %, thereafter it decreases slowly with increasing ZnO content. It is found that thermal treatments exert a pronounced effect on the resistivity of the nanocomposites. Annealed LDPE/ZnO nanocomposites exhibit lowest resistivity among the samples investigated. The resistivity begins to decrease at 1.2 vol % ZnO (critical content) followed by a step-wise decrease with increasing ZnO content. The quenched nanocomposites show the highest resistivity with ZnO critical content of 4.6 vol %. The ρ of as-prepared, annealed, and quenched LDPE/ZnO nanocomposites as a function of the (volume fraction)$^{-1/3}$, i.e., $V^{-1/3}$, is shown in Figure 9(b). It can be seen that there exists a lineal relation between log ρ and $V^{-1/3}$ for the samples investigated when ZnO content is larger than the critical volume fraction, indicating that tunneling conduction would occur in the nanocomposites investigated.[28,29]

From Figure 8, one can see that it is reasonable to assume that the filler particles are dispersed uniformly and arranged in a cubic lattice. Thus, ZnO volume content can be transform to ZnO interparticle distance using the following equation:[30]

$$l = d[(\pi/6V)^{1/3} - 1] \quad (3)$$

where V is the volume fraction of ZnO and d is the diameter of ZnO particles. Figure 9(c) shows the resisitivity of the investigated nanocomposites, ρ, as a function of interparticle distance in lower frequency region (50 Hz). The interparticle distance for LDPE/ZnO nanocomposites with 1.2, 2.8, and 4.6 vol % ZnO is determined to be ~590, 400, and 290 nm, respectively. When the interparticle distance between ZnO particles is lower than the critical distance, conduction between particles occurs via tunneling and a decrease in resistivity is produced in lower frequency region. More interestingly, compared with the critical interparticle distance for as-prepared nanocomposites, annealed nanocomposites exhibit larger, but quenched nanocomposites smaller critical interparticle distance. It is known that electron can drift more easily in amorphous phase than in crystalline phase because in the crystallization process, impurities and uncrystallizable polymer molecules are rejected out of the crystalline lamellae and finally compounded in the amorphous region. For annealed LDPE/ZnO nanocomposites, more perfect crystalline structure is formed and impurities concentration in amorphous region is higher than that of the as-prepared nanocomposites with the same ZnO loading. Accordingly, conduction between particles occurs via tunneling at larger interparticle distance. However, for quenched LDPE/ZnO nanocomposites, crystalline structure is less perfect and impurities concentration in amorphous region is lower. Accordingly, conduction between particles only occurs via tunneling at smaller interparticle distance. Hong et al.[6] investigated electrical properties of LDPE/ZnO nanocomposites. They evaluated the interparticle distance to be ~40 nm for LDPE/ZnO composites, which was much smaller than the ones determined in this article. This difference possibly rises from difference in purity of LDPE and thermal treatment as well as measurement condition (such as frequency). Yan et al.[24] investigated DC conduction of annealed polyethylene film under high electric field. They reported that the contact potentials of the metal/dielectric for polyethylene film decreases from 2.75 to 2.24 eV when the degree of crystallinity (X_c) of polyethylene increases from 52.8 to 68.2%.

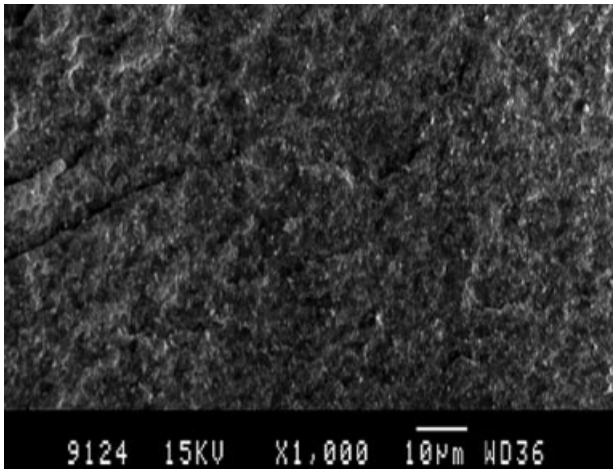

Figure 10 SEM micrograph of cryogenic fracture surfaces of as-prepared LDPE/60 vol % ZnO nanocomposite.

In eq. (3), let the interparticle distance, l, to be 0, which means that filler particles begin to connect to each other and form a network of filler particles, then the percolation concentration of filler particles can be determined to be 52 vol %. This means that when ZnO volume concentration approaches 52 vol %, a transition from isolated ZnO particles to network will occur. Figure 10 shows the SEM micrograph of cryogenic fracture surface of LDPE/60 vol % ZnO nanocomposites. Compact ZnO particle network can be readily seen throughout entire fracture surface. This indicates that ZnO particles have indeed connected each other at 60 vol % ZnO concentration. Owing to the low dielectric property of ZnO particle, there is no sharp increase in dielectric constant in the composites even when the ZnO content reaches 60 vol % (Fig. 7).

The dielectric properties of heterogeneous polymer/filler composites are well recognized to be dependent on frequency.[2–5,7,8] Figure 11 shows the dependence of dielectric constant on frequency of the quenched and annealed LDPE/ZnO nanocomposites in the range of 10^2–10^7 Hz. The dielectric constant of neat LDPE and the quenched nanocomposites with low ZnO volume content is independent of frequency.

As the ZnO volume content reaches 60 vol %, a dependence of the dielectric constant on frequency is observed, particularly at lower frequency regime ($<10^4$ Hz). Compared with the quenched nanocomposites, the frequency dependence of dielectric constant for annealed nanocomposites is more pronounced. From the above analysis, it appears that for LDPE/ZnO nanocomposite with 60 vol % ZnO content, ZnO particles have connected to each other and then formed a network throughout the nanocomposites.

It is considered that the frequency dependence of the dielectric constant of the composites at low frequency regime ($<10^4$ Hz) arises from the interfacial polarization or commonly referred to as MWS-polarization. For the quenched nanocomposites containing less than 52 vol % ZnO, the ZnO particles having the polymer/ZnO interface are dispersed independently within the LDPE matrix. As the ZnO content reaches 52 vol %, the nanoparticles begin to link together to form a network, thereby forming the ZnO/ZnO interface. The transition from the polymer/ZnO to ZnO/ZnO interface contributes to a pronounced frequency dependence of the dielectric constant at low frequency regime. The ZnO/ZnO interfacial dipole moments are considered to derive from the electrons that are trapped at the ZnO/ZnO interface.[7] Compared with the quenched nanocomposites, annealed nanocomposites exhibit perfect crystal structure. Impurity concentration at the polymer/ZnO or ZnO/ZnO interface is higher than that of the quenched nanocomposites.[24] Consequently, a pronounced frequency dependence of dielectric constant is yielded for the annealed nanocomposites.

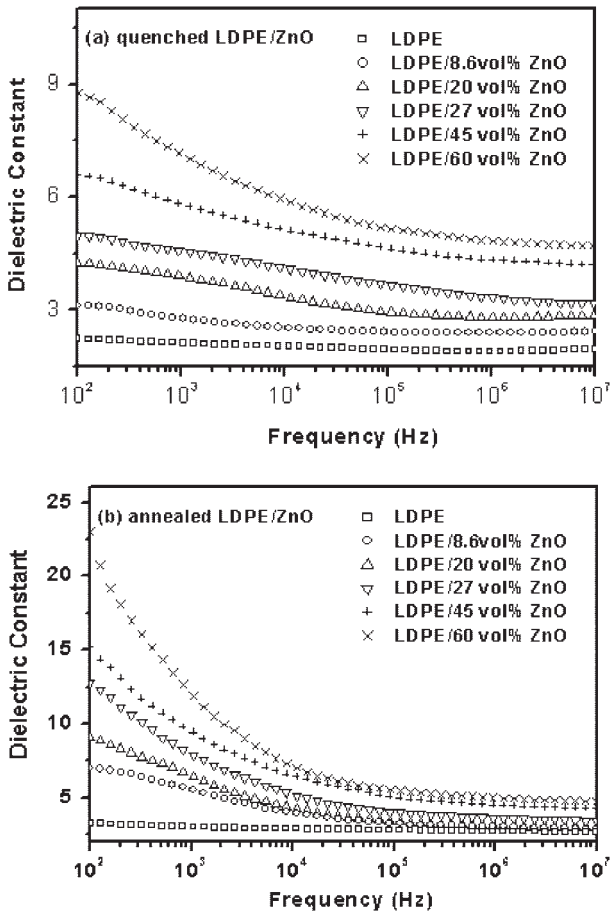

Figure 11 Plots of dielectric constant versus frequency for (a) quenched LDPE/ZnO nanocomposites and (b) annealed LDPE/ZnO nanocomposites.

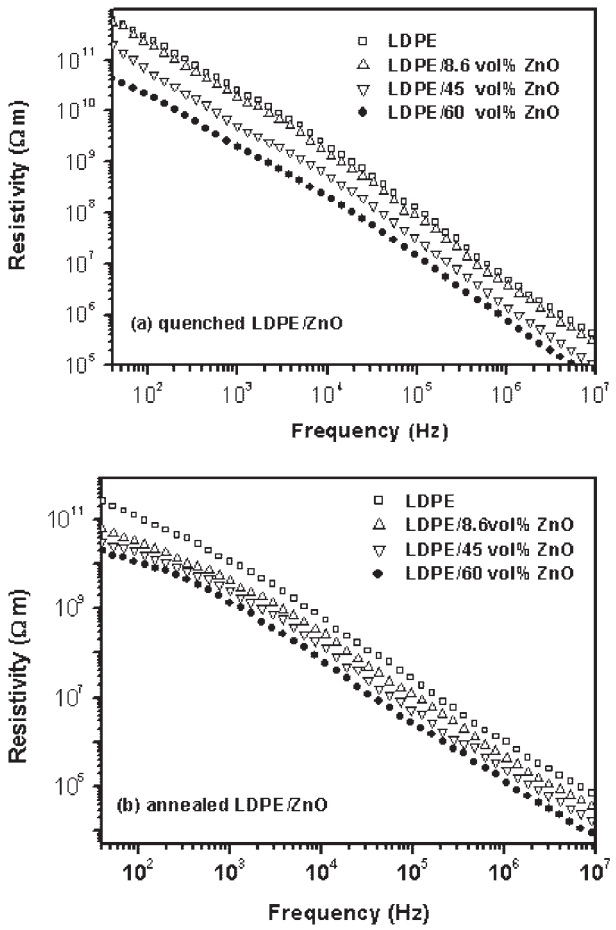

Figure 12 Plots of resistivity versus frequency for (a) quenched LDPE/ZnO nanocomposites and (b) annealed LDPE/ZnO nanocomposites.

Figure 12 shows the frequency dependence of resistivity of quenched and annealed LDPE/ZnO nanocomposites in frequency range of 40–10^7 Hz. Resistivity of the quenched nanocomposites decreases almost linearly with frequency. And the resisitivity of the nanocomposite with 60 vol % ZnO is an order of magnitude smaller than that of LDPE. A similar behavior is observed in the annealed nanocomposites in which the resistivity of LDPE/60 vol % ZnO nanocomposites is an order magnitude smaller than that of LDPE.

CONCLUSIONS

Electrical properties of LDPE/ZnO nanocomposites depend greatly on the thermal treatment processes. The degree of crystallinity of annealed LDPE/ZnO nanocomposites is higher than that of the as-prepared and quenched specimens because of the formation of more perfect crystals during annealing. The dielectric constant of annealed LDPE/ZnO nanocomposites exhibit higher dielectric constant but lower resistivity compared with those of quenched LDPE/ZnO nanocomposites at various ZnO volume content. Moreover, there is no abrupt increase in the dielectric constant with ZnO content for the as-prepared, annealed, and quenched LDPE/ZnO nanocomposites. This implies that the percolation effect is not observed for the specimens investigated. The resistivity of LDPE/ZnO nanocomposites tends to decrease when the interparticle distance is smaller than the critical value because of the tunneling conduction between adjacent ZnO particles. Comparing with the critical interparticle of as-prepared LDPE/ZnO nanocomposites, annealed LDPE/ZnO nanocomposites exhibit larger, but quenched samples show smaller critical interparticle distance. Finally, the frequency dependence of dielectric constant is much pronounced for both the annealed and quenched LDPE/ZnO nanocomposites as the ZnO volume content reaches 52 vol %, associated with the formation of ZnO network.

References

1. Cadek, M.; Coleman, J. N.; Barron, V.; Hedicke, K.; Blau, W. J Appl Phys Lett 2002, 81, 5123.
2. Nogales, A.; Broza, G.; Roslaniec, Z.; Schulte, K.; Sics, I.; Hsiao, B. S.; Sanz, A.; Garcia-Gutierrez, M. C.; Rueda, D. R.; Domingo, C.; Ezquerra, T. A. Macromolecules 2004, 37, 7669.
3. Du, F. M.; Scogna, R. C.; Zhou, W.; Brand, S.; Fischer, J. E.; Winey, K. I. Macromolecules 2004, 37, 9048.
4. Dang, Z. M.; Zhang, Y. H.; Tjong, S. C. Synth Met 2004, 146, 79.
5. Zois, H.; Mamunya, Y. P.; Apekis, L. Macromol Symp 2003, 198, 461.
6. Hong, J. I.; Schadler, L. S.; Siegel, R. W.; Martensson, E. Appl Phys Lett 2003, 82, 1956.
7. Hong, J. I.; Winberg, P.; Schadler, L. S.; Siegel, R. W. Mater Lett 2005, 59, 473.
8. Dang, Z. M.; Fan, L. Z.; Zhao, S. J.; Nan, C. W. Mater Res Bull 2003, 38, 499.
9. Lux, F. J Mater Sci 1993, 28, 285.
10. Nan, C. W. Prog Mater Sci 1993, 37, 1.
11. Zamfirescu, M.; Kavokin, A.; Gil, B.; Malpuech, G.; Kaliteevski, M. Phys Rev B 2002, 65, 161205.
12. Pearton, S. J.; Norton, D. P.; Ip, K.; Heo, Y. W.; Steiner, T. Prog Mater Sci 2005, 50, 293.
13. Anderson, R. A.; Pike, G. E. J Mater Res 2003, 18, 994.
14. Snoke, D. Science 1996, 273, 1351.
15. Hwang, C. C.; Wu, T. Y. J Mater Sci 2004, 39, 6111.
16. Hwang, C. C.; Wu, T. Y. Mat Sci Eng B: Solid 2004, 111, 197.
17. Boyle, T. J.; Bunge, S. D.; Andrews, N. L.; Matzen, L. E.; Sieg, K.; Rodriguez, M. A.; Headley, T. J Chem Mater 2004, 16, 3279.
18. Schneider, B. H.; Dickinson, E. L.; Vach, M. D.; Hoijer, J. V.; Howard, L. V. Biosens Bioelectron 2000, 15, 13.
19. Du, T.; Ilegbusi, O. J. J Mater Sci 2004, 39, 6105.
20. Yogo, T.; Nakafuku, T.; Sakamoto, W.; Hirano, S. J Mater Res 2004, 19, 651.
21. Xu, J. T.; Liang, G. D.; Fan, Z. Q. Polymer 2004, 45, 6675.
22. Xu, J. T.; Liang, G. D.; Fan, Z. Q. Polym J 2004, 36, 465.
23. Lewis, T. J. IEEE T Dielect EL In 2002, 9, 717.
24. Yan, P.; Zhou, Y. X.; Yoshimura, N. Jpn J Appl Phys 2000, 39, 3492.
25. Tjong, S. C.; Bao, S. P. J Polym Sci Part B: Polym Phys 2005, 43, 253.
26. Zheng, J. R.; Siegel, R. W.; Toney, C. G. J Polym Sci Part B: Polym Phys 2003, 41, 1033.
27. Aggarwal, S. L.; Tilley, G. P. J Polym Sci 1955, 18, 17.
28. Kilbride, B. E.; Coleman, J. N.; Fraysse, J.; Fournet, P.; Cadek, M.; Drury, A.; Hutzler, S.; Roth, S.; Blau, W. J. J Appl Phys 2002, 92, 4024.
29. Connor, M. T.; Roy, S.; Ezquerra, T. A.; Calleja, F. J. B. Phys Rev B 1998, 57, 2286
30. Wu, S. H. Polymer 1985, 26, 1855.